Comparison of GRACE Gravity Anomaly Solutions for Terrestrial Water Storage Variability in Arid and Semi-arid Botswana

Mooketsi Segobye*[1], Loago K. Motlogelwa[2], Bagadzi M. Manisa[1], Boipuso Nkwae[1], Lopang Maphale [1] and Yashon O. Ouma[1]

[1]Department of Civil Engineering, University of Botswana, PBag UB0061, Gaborone, Botswana
[2]Wetsho Tee Engineering Surveyors (Pty) Ltd, Kgale Mews, Gaborone, Botswana
segobyem@ub.ac.bw

DOI: http://dx.doi.org/10.4314/sajg.v12i1.4

Abstract

Explorations of the differences between Gravity Recovery and Climate Experiment (GRACE) solutions in local regions and basins are fundamental in determining their suitability and applicability in these environments. Because of the different mathematical inversions used by the respective processing centers, individual solutions exhibit discrepancies in terms of mass increase or loss, which makes it difficult for users to select the best model for studying terrestrial water storage anomalies (TWSAs). This study compares TWSA trends, as derived from different GRACE solutions over the arid and semi-arid Botswana (2002-2019), where both storage and flux from CSR, JPL, GFZ, TUGRAZ, AIUB, and COST-G[1] were compared. The results show that the six solutions are fairly correlated with the least correlation of R=0.829 between JPL and AIUB, and a maximum of R=0.921 between CSR and TUGRAZ at a 95% confidence level. The TWSA analyses for 2002-2019 indicate that TWS is increasing in Botswana, with the least linear trend of +0.11cm/yr detected from the TUGRAZ inversion model, and the highest linear trend at +0.43cm/year from the COST-G model. On comparing TWS with rainfall, all the solutions presented the same spatio-temporal trends as the rainfall patterns, indicating that the GRACE solutions exhibit the same responses with respect to the received rainfall. Over the 18 years investigated, the long-term rainfall trend was found to decrease, which was only detected by the TUGRAZ model in terms of the recorded equivalent water height (EWH) of -0.008cm/yr from the monthly trend observations. Overall, the AIUB inversion solution gave a better result as its signal was found to be the same as the rainfall signal.

Keywords: *GRACE gravity; terrestrial water storage anomaly; equivalent water height; semi-arid Botswana*

[1] *CSR* = Center for Space Research; *JPL* = Jet Propulsion Laboratory; *GFZ* = the German Research Center for Geosciences; *TUGRAZ* = Graz University of Techology; *AIUB* = the Astronomical Institute of the University of Bern; *COST-G* = the International Combination Service for Time-Variable Gravity Fields

Open Rubric

1. Introduction

Terrestrial water storage (TWS) comprises groundwater and above-groundwater stored as surface water, soil moisture, snow, and canopy water, and forms a significant component of the terrestrial and global hydrological cycles (Figure 1). In turn, these cycles play important roles in the Earth's climate system by controlling the energy, water, and biogeochemical fluxes (Frappart & Ramillien, 2018; Syed et al., 2008). As water storage is an integrated measure of the availability of surface and groundwater, the assessment of the water cycle and its fluxes on the continental surfaces and more so at regional scales is important in estimating water storage for water resource planning and management (Famiglietti & Rodell, 2013; Gonçalves et al., 2020; Khaki & Awange, 2019b; Khorrami & Gunduz, 2021; Ni et al., 2018; Seyoum et al., 2019). Such studies require continuous and reliable observation systems and estimation tools for the accurate determination of the water stocks available, especially in terms of groundwater, and their variability from the seasonal scale to the multi-annual temporal scale. Traditionally, the spatio-temporal heterogeneous gauge networks are used to measure in-situ river discharge rates, and less frequently, groundwater table depths (Long et al., 2016; Y. Zhou et al., 2016). However, such measurements are discrete and only present partial information on the actual water fluxes at the regional scale (Hu et al., 2019; Pavelsky, 2014; Rahaman et al., 2019; Sliwinska et al., 2019; Y. Zhou et al., 2016).

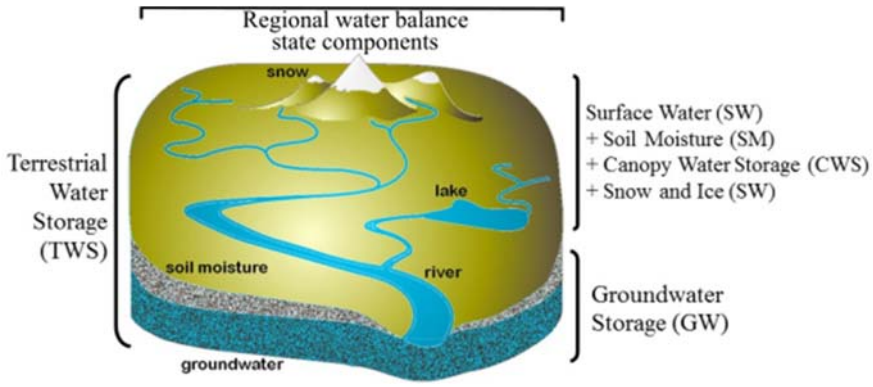

Figure 1: Terrestrial water storage (TWS) and components (Ouma et al., 2015).

To complement *in-situ* measurements, geodetic remote sensing sensors have proven capable of providing spatio-temporal near-homogeneous estimates of water variability (Lettenmaier et al., 2015; Wouters et al., 2014). Specifically, the Gravity Recovery and Climate Experiment (GRACE) twin satellite mission, can be used to estimate the terrestrial water storage change (ΔTWS) and the change in groundwater storage variations at monthly time scales with a coarse spatial resolution of approximately 300km (Khaki & Awange, 2019a).

For the estimation of fine spatio-temporal homogenous water fluxes at the watershed and regional scales, several numerical hydrological models have been used to derive the TWS and its dynamics

with river fluxes. GLDAS-NoahV2.1 and European Center for Medium-range Weather Forecast (ECMWF) Re-Analysis (ERA) interim reanalyses were used to characterize flooding over the Poyang Lake Basin (H. Zhou et al., 2018) while the WaterGAP Hydrology Model (WGHM) and the PCRaster Global Water Balance (PCR GLOBWB) model were used to study water flows and storage globally (Döll et al., 2016). These models are limited by the following: (i) the inability to adequately capture the physical processes, (ii) the finite approximations of the numerical equations used to model the processes, and (iii) the application of boundary conditions and uncertainties in the model parameters (Döll et al., 2016). Furthermore, since not all variables are validated and calibrated for the numerical hydrological models, the use of numerical models in regional estimations of the TWS variations remains a complex task (Trzaska & Schnarr, 2014). To improve on water storage and dynamics estimation modeling, satellite observations and *in situ* measurements can now be used to calibrate, validate, and correct model input parameters, as well as model outputs (Lettenmaier et al., 2015).

Spatio-temporal variations in TWS variability can be determined using the GRACE gravity anomaly-derived equivalent water thickness or height (EWH) data at regional scales (Ouma et al., 2015). GRACE is a NASA and German DLR satellite mission for mapping the gravity field of the Earth over a period of 30 days (Tapley et al., 2004). It comprises twin satellites, with the orbit of each satellite being determined by the magnitude of the Earth's gravity field. As such, local variations in this field affect the motion of the satellites by altering the distance, *d*, between the satellites, as demonstrated in Figure 2. Using mathematical inversions, the variation in the distance between the satellites is monitored and converted to variations in the gravitational field of the Earth which are called GRACE solutions (Wouters et al., 2014).

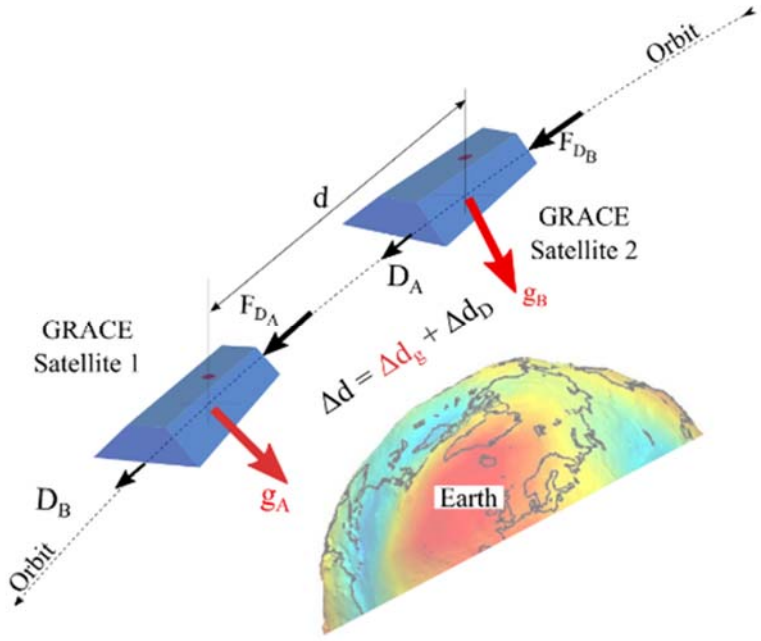

Figure 2: GRACE low-low satellite-to-satellite tracking (LL-SST) concept(modified from Dionisio et al., 2018).

While the GRACE measurements are simple, the inversion procedures are complex and coupled with errors. The GRACE solutions are derived in terms of spherical harmonic functions and as Stokes coefficients, with a spatial resolution of approximately 300km × 300km. The spatial resolution is attributed to the following factors: (i) the orbiting altitude of the satellites, (ii) the accuracy of the satellite instrument, (iii) the maximum degree of the spherical harmonics used, and (iv) the spatial scale of the filters applied to the GRACE measurements at each of the respective processing centers (Landerer & Swenson, 2012; Scanlon et al., 2016; Wouters et al., 2014). Different mathematical inversion solutions for the conversion of the GRACE gravity anomalies to EWH have been proposed. Each processing center adopts its solutions in the form of either spherical harmonic coefficients or recomputed EWH on a regular geographic grid (Watkins et al., 2015). Because of the differences in the mathematical hypotheses and solutions that are used to derive the inverse gravity fields from distance measurements determined through the GRACE satellites, the solution from each processing center is unique.

Owing to the different GRACE solution products, it is not obvious as to which product would be suitable for a given region. This study investigates the correlation and reliability of the GRACE satellite data products from the respective institutions, as listed below, for the assessment of the total terrestrial water variability in arid and semi-arid Botswana. The University of Texas at Austin's Center for Space Research (CSR); NASA's Jet Propulsion Laboratory (JPL); the German Research Centre for Geosciences Potsdam (GFZ), Institute of Geodesy at Graz University of Technology (ITSG), the Astronomical Institute of the University of Bern (AIUB), and the International Combination Service for Time-Variable Gravity Fields (COST-G) are the relevant institutions. The GRACE TWS changes are compared with rainfall data from the Department of Meteorological Services (DMS) for the 2002-2019 period in order to predict the terrestrial water variability in the country.

2. Study Area

Botswana, an arid and semi-arid country, occupies a land area of about 582,000km^2 that extends between the latitudes 18°S – 27°S and longitudes 20°E – 29.5°E (Figure 3). Up to 70% of the country is occupied by the Kalahari Desert. Hence, it is predominantly flat, with a few areas on the eastern side of the country forming rolling landscapes, thus resulting in low runoff (Farr, 2017; Segosebe & Parida, 2006). While the north-eastern portion of the country receives an annual precipitation of about 650mm, the south-western region receives an average of 250mm of precipitation per year. Almost all of the rainfall occurs during the summer months, with the winter period accounting for less than 10 percent of the annual rainfall. With a few perennial rivers, mainly located in the north-western portion of the country, the surface runoff is estimated at a mean annual rate of 50mm. In most of the central and western parts of the country, including the Kalahari region, the annual groundwater recharge

from rainfall is estimated to be lower than one millimetre/year. On the other hand, it reaches a maximum of approximately 40mm/year in small regions within the Chobe District (Lindhe et al., 2020).

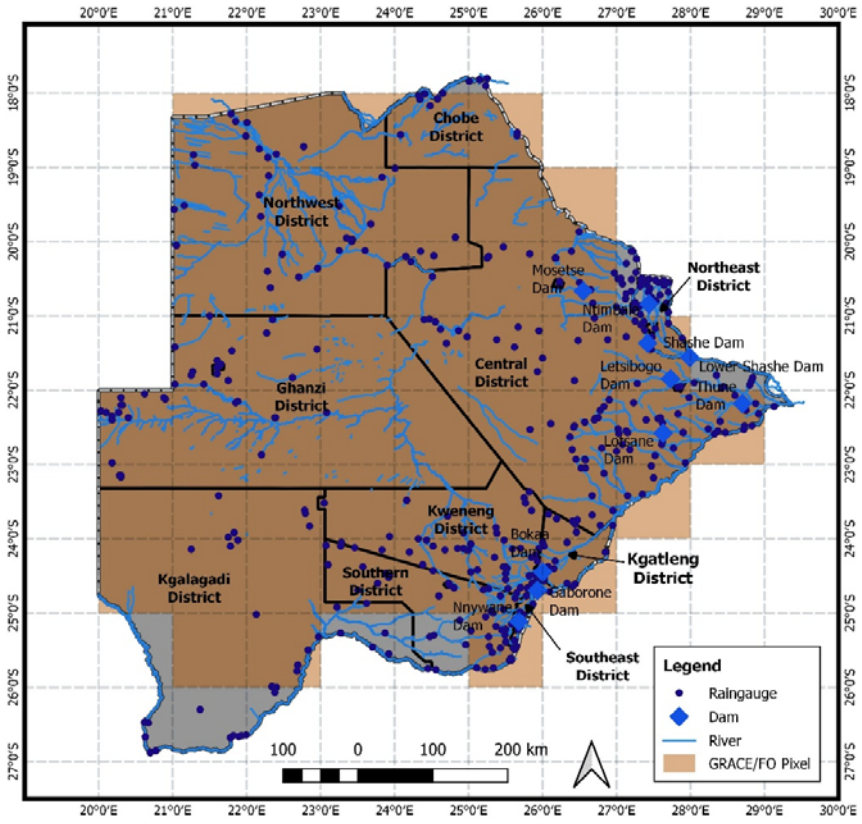

Figure 3: Location map of Botswana in southern Africa, rainfall gauge stations, and the Botswana surface water resources.

Prior to the construction of the north-south carrier (NSC) pipeline, approximately 80% of the country's water supply needs were derived from groundwater , with most rural villages and the mining industry relying wholly on groundwater (Department of Water Affairs, 2017; Farr, 2017). In accordance with the depletion of water supplies through extraction, and to cope with the ever-increasing water demands, surface water is also used to augment the groundwater supplies. The construction of reservoirs or dams for the collection and storage of ephemeral river flow facilitated this process. The dams, mainly located in the eastern part of Botswana, are connected through a NSC pipeline transfer system to provide for the possibility to transfer water to the more densely populated urban centres. The four largest dams are Dikgatlhong (400Mm^3), followed by the Gaborone (141Mm^3), Letsibgo (100Mm^3), and Thune (90Mm^3) dams, all, with the exception of the Gaborone dam, being in the north (Figure 3). However, because of the flat topography and the arid to semi-arid climate, the loss of dam water to evaporation is considerable (Ministry of Minerals Energy and Water Resources, 2012). During the drought period, the groundwater aquifers have the potential to support the dams in the eastern corridor of the country which is densely populated and characterized by fertile

soils and high levels of economic activity(Segosebe & Parida, 2006). However, the variability in the recharge of the country's aquifers has never been monitored or even quantified, especially for determining their long-term sustainability and potential capacity.

This study thus investigates not only the reliability of the GRACE solution for monitoring the TWSA in Botswana, but also presents a prediction of the TWS variability and trends from 2002 to 2019.

3. Materials and Methods

3.1. GRACE mission and data

The low earth-orbiting (LEO) twin GRACE satellites were simultaneously launched on March 17, 2002, with, their primary objective being to obtain accurate estimates of the mean and time-variable components of the variations in the earth's gravity field (Hofmann-Wellenhof & Moritz, 2006). This is determined by continuously tracking the inter-satellite range and range rate of the coplanar twin satellites, as they co-orbit at an altitude of 500km with a separation of 220km, at a micro-metre level. In this case, dual carrier phase measurements in the K (26GHz) and Ka (32GHz) frequencies of the K-band ranging (KBR) system are used (Save et al., 2016; Schmidt et al., 2008; Watkins et al., 2015) (Figure 2). With the aid of a highly precise onboard capacitive accelerometer on each spacecraft, non-gravitational forces, such as atmospheric drag, satellite perturbations, and solar radiation pressure, are measured and filtered out. The precise position and orientation of the twin satellites are measured using a GPS receiver (space-proofed multichannel, dual-frequency) and a star camera respectively located on each satellite (Rodell & Famiglietti, 1999; Tapley et al., 2004).

As gravity perturbs the orbits of the two satellites, their distance d apart changes with time (Figure 2). By measuring the overall distance variations, Δd, collected over a certain period, the map of the average gravitational field in that period can be retrieved, provided that the effect, Δd_D, of the non-gravitational forces, F_D, is properly measured by accelerometer(s) and subtracted in the data processing facilities to insulate the contribution, Δd_G, from the geopotential (Dionisio et al., 2018). The KBR measures these minute changes in the inter-satellite distance which are used to determine the strength of the gravitional field. GRACE data are divided into three levels: Level 1 data are calibrated and time-tagged in a non-destructive sense and are not available to the public; Level 2 data are spherical harmonic coefficients that can be used to generate monthly gravity field estimates; Level 3 data are EWH, representing mass anomalies on the earth.

Using the dynamic equations of their motions, an analysis of the relationships between the orbits and forces of the GRACE satellites was conducted to estimate the variations in the Earth's gravitational field. When errors in the gravity field model, the atmosphere, and ocean models are removed, the GRACE time-varying gravity field returns the non-atmospheric and non-ocean mass changes resulting from the differences in the water mass over the continental area. It provides

information on TWS changes in the large basins and regions on a seasonal or shorter time scale, (Tapley et al., 2004; Wahr et al., 1998).

In this study, as summarized in Table 1, monthly time series of time-variable Level-3 GRACE solutions from six different processing groups were used. The downloaded data products correspond to liquid EWH in centimetres on a regular grid (Figure 3).

Table 1. GRACE monthly gravity field solutions.

Gravity field solution	Solution name/ Version	Institution	Processing Strategy (Inversion Solutions)	References
AIUB	Release 02	Astronomical Institute, University of Bern	Celestial mechanics approach (pseudo-stochastic orbit parameters)	Meyer et al., 2016
COST-G	Release 01	IGFS	Hybrid solution: Combines existing solutions from COST-G analysis centers and partner analysis centers (PCs)	Jäggi et al., 2020
CSR	Release 06	CSR University of Texas	Direct approach	Save et al., 2016
GFZ	Release 06	GFZ	Direct approach	Boergens et al., 2020
JPL	Release 06	JPL	Direct approach	Watkins et al., 2015
TUGRAZ	ITSG GRACE 2018	TU Graz	Short arc approach (empirical covariances)	Kvas et al., 2019

The web-based tool (www.theGRACEplotter.com) was used to download the GRACE datasets. To derive the GRACE data from the GRACE plotter, a 10-point polygon, resulting with 52 1°× 1° of GRACE pixels, as shown in Figure 3, was used. The data were downloaded as a time series, with the 52 pixels averaged over the entire area. As the monthly downloaded GRACE data had temporal gaps, the gaps were filled by means of interpolation. At times, where there was a one month gap, data on either side of the gap were averaged(Jing et al., 2019). Where there was a gap of more than one month, linear interpolation was applied by considering the previous GRACE TWS data (Montecino et al., 2016). Annual averages were then calculated on the basis of trend analysis.

3.2. TWS anomalies emanating from GRACE

GRACE gravity data can be used to recover surface mass variability by relating changes in surface mass to changes in gravity (Figure 2). Changes in the distribution of mass in the Earth system that result from variations in water storage, result in spatio-temporal changes in the gravity potential (Ramillien et al., 2008). This temporal change in the equipotential surface can be converted into EWH (h) by using spherical harmonics, as in Equation 1 (Wahr et al., 1998).

$$h(\theta,\lambda,t) = \frac{2\pi a \rho_E}{3\rho_W} \sum_{l=0}^{l_{max}} \sum_{m=0}^{l} \frac{2l+1}{1+k_l} \bar{P}_{lm}(\cos\theta)\left[\Delta\bar{C}_{lm}(t)\cos m\lambda + \Delta\bar{S}_{lm}(t)\sin m\lambda\right] \quad [1]$$

for month t, θ = colatitude; ρ_E = average density of the Earth; ρ_W = density of water, λ = longitude; R = mean radius of the earth, $\bar{P}_{lm}$= normalized associated Legendre functions of degree l and order m, and $\Delta\tilde{C}_{lm}$ and $\Delta\tilde{S}_{lm}$ = the residual surface density coefficients, which define the filters for the conversion of geoid variations to h (cm) (Equations 2-3):

$$\Delta\tilde{C}_{lm}(t) = \frac{\rho_E}{3\rho_w}\frac{2l+1}{1+k_l}\Delta\bar{C}_{lm}(t) \quad [2]$$

$$\Delta\tilde{S}_{lm}(t) = \frac{\rho_E}{3\rho_w}\frac{2l+1}{1+k_l}\Delta\bar{S}_{lm}(t) \quad [3]$$

where k_l = load Love number for degree l. $\Delta\tilde{C}_{lm}$, and $\Delta\tilde{S}_{lm}$ = the residual Stokes coefficients, defined as Equations 4 and 5:

$$\Delta\bar{C}_{lm}(t) = \bar{C}_{lm}(t) - \frac{1}{N}\sum_{i=1}^{N}(\bar{C}_{lm})_i \quad [4]$$

$$\Delta\bar{S}_{lm}(t) = \bar{S}_{lm}(t) - \frac{1}{N}\sum_{i=1}^{N}(\bar{S}_{lm})_i \quad [5]$$

where $\bar{C}_{lm}$ and $\bar{S}_{lm}$ = the long-term means of the Stokes coefficients and N = the total number of monthly (i^{th}) solutions. The mean long-term Stokes coefficients representing the mean static field are removed as they are dominated by the static density distribution within the solid Earth. This implies that the contributions from the mean stored water are also removed, and in terms of the water storage anomalies, only the time variable component of the water storage is recovered(Ditmar, 2018; Swenson & Wahr, 2002; Wahr et al., 1998).

3.3. Precipitation data

In comparing the precipitation and TWS cycles, mean monthly measured rainfall figures from 28 gauging stations within Botswana were considered for the 2002-2019 study duration. Only gauging stations which had data gaps of less than one month were used. The proportion of data gaps in each of the chosen gauging stations amounted to less than one percent (1%). The global monthly accumulated precipitation from Tropical Rainfall Measuring Mission (TRMM) products with 0.25° × 0.25° spatial resolution were used to fill in any missing precipitation data in the gauge data series. For comparison with the GRACE data, the TRMM precipitation data were filtered using the Gaussian

To evaluate the different EWH time series, they were compared with the mean annual rainfall over the study period. The two time series, EWH and annual rainfall, were compared for similarities by using dynamic time warping (DTW) (Cheong, 2019) and Pearson's correlation coefficient (Moriasi et al., 2007; Yin et al., 2021). For DTW, the two signals were first standardized so that they had a

mean and standard deviation of 0 and 1 respectively. The same analysis was also conducted for the detrended time analysis.

4. Results and Discussions

4.1. Correlational analysis and inter-annual EWH changes

A heatmap plot of the correlations among the respective solutions is presented in Figure 4. The correlations depict the GRACE solutions as having high correlations, with the least correlation between JPL and AIUB being R = 0.827, and the highest between CSR and TUGRAZ being R = 0.921. Generally, AIUB was found to have the lowest correlations with all of the other five solutions.

Table 2 shows the mean annual rainfall and the corresponding EWH values for all of the solutions. The computed inter-annual changes show that the highest inter-annual increase in EWH, ranging between +9.12cm and +11.66cm, was recorded in 2006, 2014, and 2017. The least EWH was observed in 2007 and 2018, while the largest changes, as shown by the yellow highlights in Table 2, were observed in 2006 and 2017. It can also be noted from Table 2 that even though they are using the same GRACE data, the institutions can produce different EWH data. These can be attributed to the different processing strategies that are used to derive EWH from GRACE raw data (see Table 1). In some cases, some solutions will present with an increased (positive) EWH while others will show a decrease (negative) in EWH.

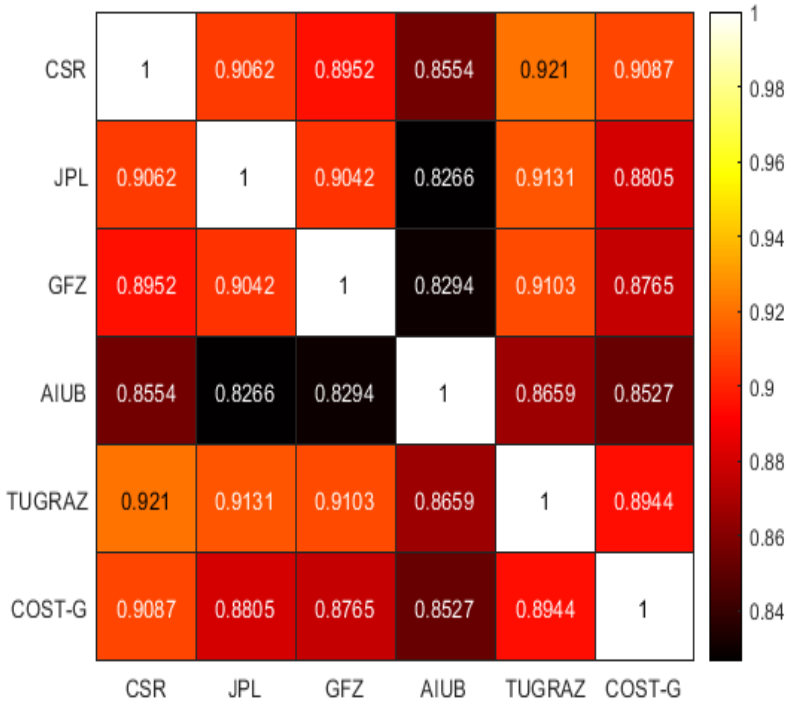

Figure 4: Heatmap with correlation coefficients.

Table 2: Annual rainfall and annual EWH and the corresponding inter-annual changes.

Date	Mean Rainfall	Mean GRACE EWH (cm)						Mean Rainfall	Inter-annual changes in EWH (cm)					
		CSR	JPL	GFZ	AIUB	COSTG	TUG		CSR	JPL	GFZ	AIUB	COSTG	TUG
2002	28.01	-2.00	-2.74	-2.81	-5.00	-2.00	-0.71							
2003	31.82	-3.86	-5.7	-3.97	-5.98	-4.51	-4.2	3.81	-1.86	-2.96	-1.16	-0.98	-2.51	-3.49
2004	35.47	-3.31	-2.23	0.71	-1.32	-2.12	-2.2	3.65	0.55	3.47	4.68	4.66	2.39	2.00
2005	28.79	-4.86	-4.67	-3.68	-4.92	-5.2	-5.2	-6.68	-1.55	-2.44	-4.39	-3.6	-3.08	-3.00
2006	51.46	4.65	4.96	4.47	4.81	4.3	3.9	22.67	9.51	9.63	8.15	9.73	9.5	9.1
2007	27.46	-2.83	-2.76	-2.64	-2.65	-3.24	-3.1	-24.00	-7.48	-7.72	-7.11	-7.46	-7.54	-7.00
2008	39.78	0.11	-0.13	0.93	0.644	0.42	1.24	12.32	2.94	2.63	3.57	3.294	3.66	4.34
2009	47.65	2.86	2.38	1.73	2.27	1.72	2.06	7.87	2.75	2.51	0.8	1.626	1.3	0.82
2010	41.92	2.89	2.74	2.28	2.51	2.35	2.69	-5.73	0.03	0.36	0.55	0.24	0.63	0.63
2011	36.10	4.61	3.57	3.44	3.27	3.17	3.41	-5.82	1.72	0.83	1.16	0.76	0.82	0.72
2012	26.45	1.18	0.23	-0.47	0.19	0.48	1.76	-9.65	-3.43	-3.34	-3.91	-3.08	-2.69	-1.65
2013	24.80	-1.05	-1.76	-2.00	-3.09	-2.37	-1.59	-1.65	-2.23	-1.99	-1.53	-3.28	-2.85	-3.35
2014	34.34	5.01	4.33	5.48	6.03	5.38	5.61	9.54	6.06	6.09	7.48	9.12	7.75	7.2
2015	17.82	0.57	0.07	0.66	-1.05	-1.33	-0.05	-16.52	-4.44	-4.26	-4.82	-7.08	-6.71	-5.66
2016	25.12	-1.9	1.73	-2.23	-1.92	-2.11	-1.52	7.3	-2.47	1.66	-2.89	-0.87	-0.78	-1.47
2017	35.25	9.7	9.47	6.68	4.02	9.55	6.02	10.13	11.6	7.74	8.91	5.94	11.66	7.54
2018	26.15	-0.41	0.14	-0.67	-1.06		-1.56	-9.1	-10.11	-9.33	-7.35	-5.08	-9.55	-7.58
2019	22.20	-5.57	-6.22	-4.21	-3.99		-5.99	-3.95	-5.16	-6.36	-3.54	-2.93	0.00	-4.43

5. Mean annual GRACE solutions and rainfall patterns

Figure 6 presents the results of the comparison of mean annual rainfall and the mean linear EWH before the detrending of the GRACE data. The long-term trend of the annual rainfall shows a declining rainfall between 2002 and 2019, whereas the long-term trends for EWH show increases for all the solutions. Thus, in terms of long-term trends, the two signals capture opposite trends between rainfall and the mean annual EWH. However, the differences are small, with a decrease observed in rainfall and a marginal increase in the TWS variability. From Figure 6, the linear trends show that the change in TWS per year from TUGRAZ is least, at +0.11cm/year, and highest from COST-G, at +0.43cm/year.

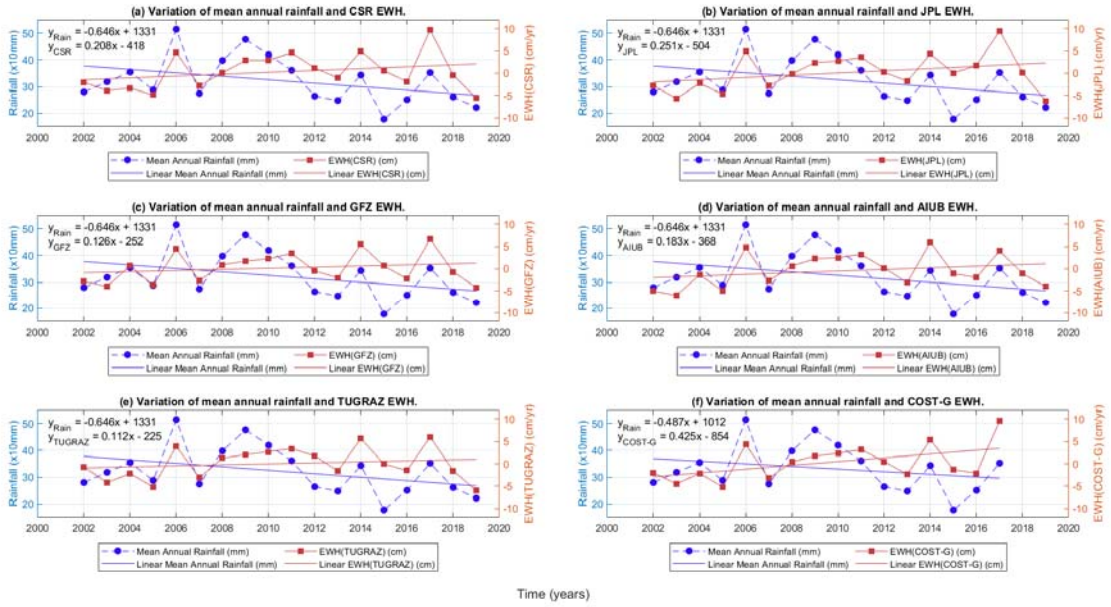

Figure 5: Relationship between annual rainfall and the EWH data presented by (a) CSR, (b) JPL, (c) GFZ, (d) AIUB, (e) TUGRAZ and (f) COST-G.

Compared with the linear trend, the de-trended annual EWH variations show the same irregular pattern as the rainfall data (Figure 7). There were only marginal differences at three time epochs for all solutions. Between 2002 and 2003, rainfall showed an increase of +38.1mm, with all EWH solutions decreasing. AIUB showed the lowest decrease of -0.98cm, and TUGRAZ the highest decrease of -3.49cm. In this period, AIUB has presented the closest signal to rainfall. Another period where the pattern differed was in the two-year period between 2009 and 2011, with the rainfall decreasing and the EWH increasing. From 2015 to 2016, rainfall showed an increase of

+73mm, while at the same time EWH decreased, with the exception of JPL, which presented an increase of +1.66cm in EWH.

A comparison of the annual linear EWH (Figure 6) and the detrended annual EWH (Figure 7) leads to the conclusion that the true relationship between rainfall and the EWH in Botswana is best derived from the detrended data.

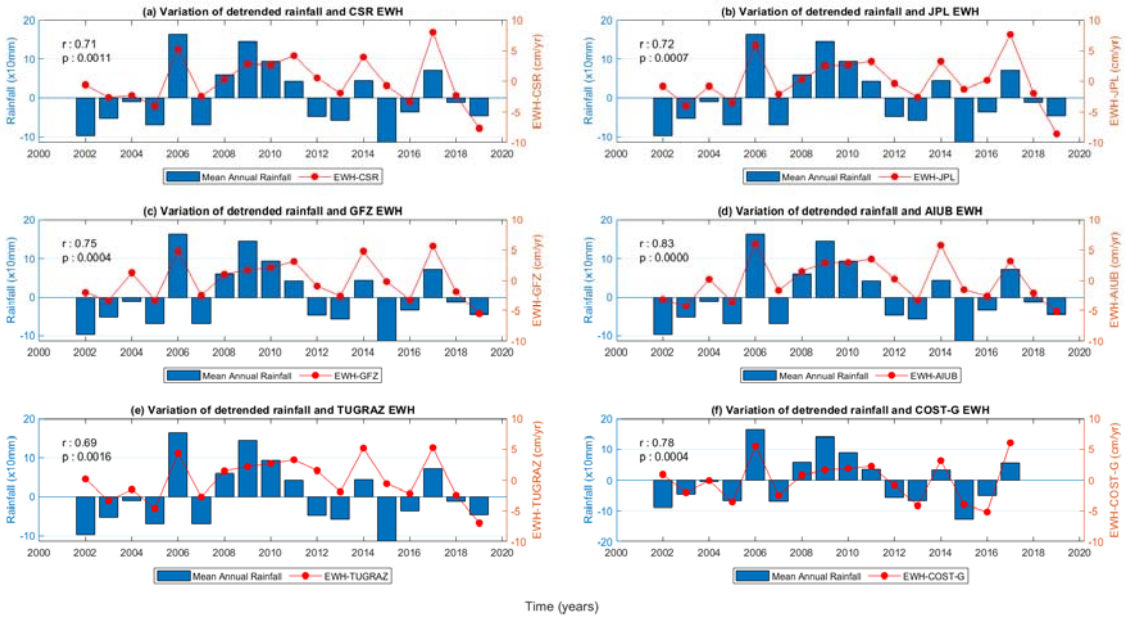

Figure 6: Detrended mean annual rainfall and EWH data as provided by (a) CSR, (b) JPL, (c) GFZ, (d) AIUB, (e) TUGRAZ, and (f) COST-G

To further evaluate the solutions, the EWH and rainfall signals were assessed for similarities using dynamic time warping (DTW), Pearson's correlation coefficient, and the p-value. For DTW, the data were standardized before processing; this is because the two signals were measured with different units. Hence standardization moderates the magnitude of the rainfall signals. The similarities were evaluated for the full-time and detrended time series. The shortest distance between rainfall and EWH is for AIUB. The Pearson correlation coefficient was calculated on the basis of the detrended data. As shown by the high correlation coefficient and the low *p*-value, the results indicate that the AIUB data presents with a significant association between EWH and rainfall (Table 4).

Table 4: Dynamic time warping (DTW) and Pearson's correlation coefficient (r) between rainfall and GRACE solutions over Botswana. DTW was calculated for the standardized data.

GRACE solution	Full time series			Detrended component		
	DTW	R	*p*-value	DTW	R	*p*-value
EWH-CSR	12.49	0.518	0.028	9.95	0.71	0.0011
EWH-JPL	12.49	0.501	0.034	9.95	0.72	0.0007
EWH-GFZ	11.20	0.596	0.009	9.59	0.75	0.0004
EWH-AIUB	11.23	0.627	0.005	8.04	0.83	0.0000
EWH-COST-G	12.07	0.511	0.043	8.05	0.77	0.0004
EWH -TUG	12.30	0.559	0.015	9.90	0.69	0.0004

Table 4 also shows that AIUB presents with the highest correlation and the shortest distance for both the full time series and the detrended component of the time series. GFZ then follows for the full series, with the lowest similarity being for JPL. On the detrended component, COST-G follows AIUB with a DTW of 8.04 and an r of 0.77; while the lowest similarity is from TUGRAZ, with an r of 0.69. Despite these observations, all solutions in terms of the p-values were found to be significant, with the p-values ranging from 0.0000 to 0.0011 for the detrended time series and 0.015 to 0.028 for the full time series.

6. Conclusions

This study compared TWS from six GRACE solutions over Botswana between April 2002 and December 2019. All the solutions presented a high degree of similarity, with the lowest correlation of 0.82 being between JPL and AIUB. In comparison with rainfall, the linear trends show marginal differences, with rainfall decreasing and TWS increasing. The results show that the six solutions are fairly correlated with the least correlation of r=0.8294 being between JPL and AIUB and the maximum correlation, r=0.921, being between CSR and TUGRAZ. The TWSA analyses from 2002-2019 indicate that the TWS is increasing in Botswana with the least linear trend of +0.11cm/year detected from the TUGRAZ inversion model and the highest linear trend of +0.43cm/year from the COST-G model. However, the positive/increase and negative/decrease in EWH by the different inversion solutions for the same data year show that the solutions include discrepancies and should be evaluated prior to use. In comparison with rainfall, all solutions present with a correlation coefficient of more than 0.5, thus showing that the two signals have nearly the same response to terrestrial water availability at a 95% confidence level, with all p-values being less than 0.034. Observations over the 18 years indicate that the overall rainfall trend is decreasing. However, in terms of the recorded EWH of -0.008cm/yr from the monthly trend

observations, only the TUGRAZ model was able to detect this phenomenon. From the general trend analysis, it can be concluded that all the solutions can be used to study the variability of TWS in arid and semi-arid Botswana. This conclusion is based on the fact that, as shown by the low DTW and the high R, the data pertaining to these solutions are similar to those for the rainfall. However, for TWS quantifications, users should carry out further analyses to determine the optimal inversion solutions for the study area. Because of the similarities in the solutions, this study recommends that the solutions be averaged to improve the quality of the TWSA and to compensate for the missing data from the different solutions.

7. References

Boergens, E., Dobslaw, H., & Dill, R. (2020). *COST-G GravIS RL01 Continental Water Storage Anomalies. V. 0004. GFZ Data Services*. https://doi.org/https://doi.org/10.5880/COST-G.GRAVIS_01_L3_TWS

Cheong, J. H. (2019). *Four ways to quantify synchrony between time series data*. https://jinhyuncheong.com/jekyll/update/2019/05/16/Four_ways_to_qunatify_synchrony.html

D. N. Moriasi, J. G. Arnold, M. W. Van Liew, R. L. Bingner, R. D. Harmel, & T. L. Veith. (2007). Model Evaluation Guidelines for Systematic Quantification of Accuracy in Watershed Simulations. *Transactions of the ASABE*, *50*(3), 885–900. https://doi.org/10.13031/2013.23153

Department of Water Affairs. (2017). *Botswana Water Accounting Report 2015/16*.

Dionisio, S., Anselmi, A., Bonino, L., Cesare, S., Massotti, L., & Silvestrin, P. (2018). The "Next Generation Gravity Mission": challenges and consolidation of the system concepts and technological innovations. *SpaceOps Conference*. https://doi.org/10.2514/6.2018-2495

Ditmar, P. (2018). Conversion of time-varying Stokes coefficients into mass anomalies at the Earth's surface considering the Earth's oblateness. *Journal of Geodesy*, *92*(12), 1401–1412. https://doi.org/10.1007/s00190-018-1128-0

Döll, P., Douville, H., Güntner, A., Müller Schmied, H., & Wada, Y. (2016). Modelling Freshwater Resources at the Global Scale: Challenges and Prospects. *Surveys in Geophysics*, *37*(2), 195–221. https://doi.org/10.1007/s10712-015-9343-1

Famiglietti, J. S., & Rodell, M. (2013). Water in the Balance. *Science*, *340*(6138), 1300–1301. https://doi.org/10.1126/science.1236460

Farr, J. L. (2017). *Groundwater Monitoring Assessment Study Botswana*.

Frappart, F., & Ramillien, G. (2018). Monitoring groundwater storage changes using the Gravity Recovery and Climate Experiment (GRACE) satellite mission: A review. In *Remote Sensing* (Vol. 10, Issue 6). MDPI AG. https://doi.org/10.3390/rs10060829

Gonçalves, R. D., Stollberg, R., Weiss, H., & Chang, H. K. (2020). Using GRACE to quantify the depletion of terrestrial water storage in Northeastern Brazil: The Urucuia Aquifer System. *Science of the Total Environment*, *705*. https://doi.org/10.1016/j.scitotenv.2019.135845

Hofmann-Wellenhof, B., & Moritz, H. (2006). *Physical Geodesy* (2nd ed.). Springer Vienna. https://doi.org/10.1007/978-3-211-33545-1

Hu, K. X., Awange, J. L., Kuhn, M., & Saleem, A. (2019). Spatio-temporal groundwater variations associated with climatic and anthropogenic impacts in South-West Western Australia. *Science of the Total Environment*, *696*, 133599. https://doi.org/10.1016/j.scitotenv.2019.133599

Jäggi, A., Meyer, U., Lasser, M., Jenny, B., Lopez, T., Flechtner, F., Dahle, C., Förste, C., Mayer-Gürr, T., Kvas, A., Lemoine, J.-M., Bourgogne, S., Weigelt, M., & Groh, A. (2020). *International Combination Service for Time-Variable Gravity Fields (COST-G)*. https://doi.org/10.1007/1345_2020_109

Jing, W., Zhang, P., & Zhao, X. (2019). A comparison of different GRACE solutions in terrestrial water storage trend estimation over Tibetan Plateau. *Scientific Reports*, *9*(1), 1–10. https://doi.org/10.1038/s41598-018-38337-1

Khaki, M., & Awange, J. L. (2019a). Improved remotely sensed satellite products for studying Lake Victoria's water storage changes. *Science of the Total Environment*, *652*, 915–926. https://doi.org/10.1016/j.scitotenv.2018.10.279

Khaki, M., & Awange, J. L. (2019b). The application of multi-mission satellite data assimilation for studying water storage changes over South America. *Science of the Total Environment*, *647*, 1557–1572. https://doi.org/10.1016/j.scitotenv.2018.08.079

Khorrami, B., & Gunduz, O. (2021). Evaluation of the temporal variations of groundwater storage and its interactions with climatic variables using GRACE data and hydrological models: A study from Turkey. *Hydrological Processes*, *35*(3), 1–13. https://doi.org/10.1002/hyp.14076

Kvas, A., Behzadpour, S., Ellmer, M., Klinger, B., Strasser, S., Zehentner, N., & Mayer-Gürr, T. (2019). ITSG-Grace2018: Overview and Evaluation of a New GRACE-Only Gravity Field Time Series. *Journal of Geophysical Research: Solid Earth*, *124*(8), 9332–9344. https://doi.org/10.1029/2019JB017415

Landerer, F. W., & Swenson, S. (2012). Accuracy of scaled GRACE terrestrial water storage estimates. *Water Resources Research*, *48*(4). https://doi.org/10.1029/2011WR011453

Lettenmaier, D. P., Alsdorf, D., Dozier, J., Huffman, G. J., Pan, M., & Wood, E. F. (2015). Inroads of remote sensing into hydrologic science during the WRR era. *Water Resources Research*, *51*(9), 7309–7342. https://doi.org/10.1002/2015WR017616

Lindhe, A., Rosén, L., Johansson, P. O., & Norberg, T. (2020). Dynamic water balance modelling for risk assessment and decision support on MAR potential in Botswana. *Water (Switzerland)*, *12*(3), 1–13. https://doi.org/10.3390/w12030721

Long, D., Chen, X., Scanlon, B. R., Wada, Y., Hong, Y., Singh, V. P., Chen, Y., Wang, C., Han, Z., & Yang, W. (2016). Have GRACE satellites overestimated groundwater depletion in the Northwest India Aquifer? *Scientific Reports*, *6*. https://doi.org/10.1038/SREP24398

Meyer, U., Jäggi, A., Jean, Y., & Beutler, G. (2016). AIUB-RL02: an improved time-series of monthly gravity fields from GRACE data. *Geophysical Journal International Geophys. J. Int*, *205*, 1196–1207. https://doi.org/10.1093/gji/ggw081

Ministry of Minerals Energy and Water Resources. (2012). *Botswana National Water Policy*.

Montecino, H. C., Staub, G., Ferreira, V. G., & Parra, L. B. (2016). Monitoring Groundwater Storage in Northern Chile Based on Satellite Observations and Data Simulation. *Boletim de Ciências Geodésicas*, *22*(1), 1–15. https://doi.org/10.1590/s1982-21702016000100001

Ni, S., Chen, J. L., Wilson, C. R., Li, J., Hu, X., & Fu, R. (2018). Global Terrestrial Water Storage Changes and Connections to ENSO Events. In *Surveys in Geophysics* (Vol. 39, Issue 1, pp. 1–22). Springer Netherlands. https://doi.org/10.1007/s10712-017-9421-7

Ouma, Y. O., Aballa, D. O., Marinda, D. O., Tateishi, R., & Hahn, M. (2015). Use of GRACE time-variable data and GLDAS-LSM for estimating groundwater storage variability at small basin scales: a case study of the Nzoia River Basin. *International Journal of Remote Sensing*, *36*(22), 5707–5736. https://doi.org/10.1080/01431161.2015.1104743

Pavelsky, T. M. (2014). Using width-based rating curves from spatially discontinuous satellite imagery to monitor river discharge. *Hydrological Processes*, n/a-n/a. https://doi.org/10.1002/hyp.10157

Rahaman, M. M., Thakur, B., Kalra, A., Li, R., & Maheshwari, P. (2019). Estimating high-resolution groundwater storage from GRACE: A random forest approach. *Environments - MDPI*, *6*(6). https://doi.org/10.3390/environments6060063

Ramillien, G., Famiglietti, J. S., & Wahr, J. (2008). Detection of continental hydrology and glaciology Signals from GRACE: A review. *Surveys in Geophysics*, *29*(4–5), 361–374. https://doi.org/10.1007/s10712-008-9048-9

Rodell, M., & Famiglietti, J. S. (1999). Detectability of variations in continental water storage from satellite observations of the time dependent gravity field. *Water Resources Research*, *35*(9), 2705–2723. https://doi.org/10.1029/1999WR900141

Save, H., Bettadpur, S., & Tapley, B. D. (2016). High-resolution CSR GRACE RL05 mascons. *Journal of Geophysical Research: Solid Earth*, *121*(10), 7547–7569. https://doi.org/10.1002/2016JB013007

Scanlon, B. R., Zhang, Z., Save, H., Wiese, D. N., Landerer, F. W., Long, D., Longuevergne, L., & Chen, J. L. (2016). Global evaluation of new GRACE mascon products for hydrologic applications. *Water Resources Research*, *52*(12), 9412–9429. https://doi.org/10.1002/2016WR019494

Schmidt, R., Flechtner, F., Meyer, U., Neumayer, K. H., Dahle, C., König, R., & Kusche, J. (2008). Hydrological signals observed by the GRACE satellites. In *Surveys in Geophysics* (Vol. 29, Issues 4–5, pp. 319–334). https://doi.org/10.1007/s10712-008-9033-3

Segosebe, E., & Parida, B. P. (2006). Water demand management in Botswana Challenges of a diminishing resource. *International Journal of Sustainable Development and Planning*, *1*(3), 317–325. https://doi.org/10.2495/SDP-V1-N3-317-325

Seyoum, W., Kwon, D., & Milewski, A. (2019). Downscaling GRACE TWSA Data into High-Resolution Groundwater Level Anomaly Using Machine Learning-Based Models in a Glacial Aquifer System. *Remote Sensing*, *11*(7), 824. https://doi.org/10.3390/rs11070824

Sliwinska, J., Birylo, M., Rzepecka, Z., & Nastula, J. (2019). Analysis of groundwater and total water storage changes in poland using GRACE observations, in-situ data, and various assimilation and climate models. *Remote Sensing*, *11*(24), 1–42. https://doi.org/10.3390/rs11242949

Swenson, S., & Wahr, J. (2002). Methods for inferring regional surface-mass anomalies from Gravity Recovery and Climate Experiment (GRACE) measurements of time-variable gravity. In *Journal of Geophysical Research: Solid Earth* (Vol. 107, Issue B9, p. ETG 3-1-ETG 3-13). https://doi.org/10.1029/2001jb000576

Syed, T. H., Famiglietti, J. S., Rodell, M., Chen, J. L., & Wilson, C. R. (2008). Analysis of terrestrial water storage changes from GRACE and GLDAS. *Water Resources Research*, *44*(2). https://doi.org/10.1029/2006WR005779

Tapley, B. D., Bettadpur, S., Ries, J. C., Thompson, P. F., & Watkins, M. M. (2004). GRACE Measurements of Mass Variability in the Earth System. *Science*, *305*(5683), 503–505. https://doi.org/10.1126/science.1099192

Tapley, B. D., Bettadpur, S., Watkins, M. M., & Reigber, C. (2004). The gravity recovery and climate experiment: Mission overview and early results. *Geophysical Research Letters*, *31*(9), n/a-n/a. https://doi.org/10.1029/2004GL019920

Trzaska, S., & Schnarr, E. (2014). A review of downscaling methods for climate change projections. *United States Agency for International Development by Tetra Tech ARD*, *September*, 1–42.

Wahr, J., Molenaar, M., & Bryan, F. (1998). Time variability of the Earth's gravity field: Hydrological and oceanic effects and their possible detection using GRACE. *Journal of Geophysical Research: Solid Earth*, *103*(B12), 30205–30229. https://doi.org/10.1029/98JB02844

Watkins, M. M., Wiese, D. N., Yuan, D. N., Boening, C., & Landerer, F. W. (2015). Improved methods for observing Earth's time variable mass distribution with GRACE using spherical cap mascons. *Journal of Geophysical Research: Solid Earth*, *120*(4), 2648–2671. https://doi.org/10.1002/2014JB011547

Wouters, B., Bonin, J. A., Chambers, D. P., Riva, R. E. M., Sasgen, I., & Wahr, J. (2014). GRACE, time-varying gravity, Earth system dynamics and climate change. *Reports on Progress in Physics*, *77*(11). https://doi.org/10.1088/0034-4885/77/11/116801

Yin, W., Fan, Z., Tangdamrongsub, N., Hu, L., & Zhang, M. (2021). Comparison of physical and data-driven models to forecast groundwater level changes with the inclusion of GRACE – A case study over the state of Victoria, Australia. *Journal of Hydrology*, *602*(August), 126735. https://doi.org/10.1016/j.jhydrol.2021.126735

Zhou, H., Luo, Z., Tangdamrongsub, N., Zhou, Z., He, L., Xu, C., Li, Q., & Wu, Y. (2018). Identifying flood events over the Poyang Lake Basin using multiple satellite remote sensing observations, hydrological models and in situ data. *Remote Sensing*, *10*(5). https://doi.org/10.3390/rs10050713

Zhou, Y., Jin, S., Tenzer, R., & Feng, J. (2016). Water storage variations in the Poyang Lake Basin estimated from GRACE and satellite altimetry. *Geodesy and Geodynamics*, *7*(2), 108–116. https://doi.org/10.1016/j.geog.2016.04.003